IOP Conference Series: Materials Science and Engineering

PAPER • OPEN ACCESS

Synthesis, morphological, optical properties of functionalized $La_{0.33}Ca_{0.67}MnO_3$ for antibacterial therapy

To cite this article: Abiola Edobor-Osoh *et al* 2019 *IOP Conf. Ser.: Mater. Sci. Eng.* **509** 012040

IOP Conf. Series: Materials Science and Engineering **509** (2019) 012040 doi:10.1088/1757-899X/509/1/012040

Synthesis, morphological, optical properties of functionalized $La_{0.33}Ca_{0.67}MnO_3$ for antibacterial therapy

Abiola Edobor-Osoh[1,3*], Benedict Iserom Ita[1, 2], Kolawole Oluseyi Ajanaku[1], P. de la Presa[3], Cyril O. Ehi-Eromosele[1], S. J. Olorunsola[4], F. E. Owolabi[1]

[1] Department of Chemistry, Covenant University, Ota, Ogun State, Nigeria.
[2] Department of Pure and Applied Chemistry, University of Calabar, Cross River State, Nigeria
[3] Applied Magnetism Institute, UCM-ADIF-CSIC, 28230, Las Rozas, Spain.
[4] Department of Biological Sciences, Covenant University, Ota, Ogun State, Nigeria
* Corresponding author: abiola.edobor@covenantuniversity.edu.ng

Abstract. A functionalized paramagnetic manganite $La_{0.33}Ca_{0.67}MnO_3$ was investigated for its morphological, optical and antimicrobial properties. The manganite was capped by using a citrate ligand. The UV-visible spectrophotometer was used in monitoring the optical bands of the metal-citrate complex. It was observed to absorb in the visible region. The metal-citrate was reacted with a biologically active ligand (*N*-(3-nitrophenyl)-3-phenyl-2-(phenylsulfonamido) propanamide). The optical bands observed from the metal-citrate were used in monitoring the reaction between the metal-citrate and N-(3-nitrophenyl)-3-phenyl-2-(phenylsulfonamido) propanamide). The morphological property of the product formed was determined using SEM-EDAX. The effect of the complex formed on the organic ligand, N-(3-nitrophenyl)-3-phenyl-2-(phenylsulfonamido) propanamide) was determined using ^{1}H and ^{13}C NMR. The bacterial inhibitory property of the metal-citrate- *N*-(3-nitrophenyl)-3-phenyl-2-(phenylsulfonamido) propanamide) complex was determined against *Pseudomonas aeruginosa* and *Staphylococcus auerus*. It was observed to inhibit the growth of *Staphylococcus aureus* only. The biological activities of the metal-citrate *N*-(3-nitrophenyl)-3-phenyl-2-(phenylsulfonamido) propanamide) suggest its use as an alternative antibacterial therapy.
Keywords: Pseudomonas *aeruginosa*, *Staphylococcus aureus*, Functionalization, Manganite and Nanoparticles

1. Introduction

Nanoparticle in recent times has been indispensably used in medicine and biotechnology in drug delivery and bactericidal drugs [1-3]. Nanomedicine introduces an approach to overcome challenges of recent traditional drug delivery systems based on the synthesis, development, fabrication and modification of nanostructures. There are various types of nanoparticle systems that have been tried as potential drug delivery systems including, metal containing nanoparticles, biodegradable polymeric nanoparticles [4], nanogels, solid lipid nanoparticles (SLN), nanoliposomes [5].

Functionalization of nanoparticles is a very important phenomenon that defines its use in nanomedicine. Functionalized nanoparticles have been attested to have multifunctional properties that enhance its efficacy in various treatments such as cancer therapy [6], drug delivery [7], magnetic resonance imaging [8] etc. The surface of nanoparticles has been covalently bonded to small molecules which include small biocompatible ligands, dyes and silica [9]. PEG coated gold nanorods have been

used for murine tumor tissues by passive targeting mechanism [10]. Manganites have been famous for their ability to be easily modified, despite their various properties and uses the ability to use them in biomedicine has been very limited, hence, the functionalization of the nanoparticles [11]. Although the surface of manganites have been modified using a number of ligands and used in detection [12] and treatment of various diseases [13], however to date no attempt has been made to functionalize manganites using a sulphonamide despite the fact that they are known antibacterial agents, the use of manganites gives the opportunity for target therapeutic drug delivery to infested cells.

Therefore, this research focuses on the functionalization La0.33Ca0.67MnO3 using N-(3-nitrophenyl)-3-phenyl-2-(phenylsulfonamido)propanamide as the organic ligand to improve the antimicrobial activity of the functionalized nanoparticle against Pseudomonas aeruginosa and Staphylococcus aureus.

2. Materials and Methods

La_2O_3, $CaCO_3$, $MnCO_3$, trisodium citrate, ethylene glycol, citric acid and phosphate buffer were obtained from Sigma-Adrich (USA) and they were used without further purification. The ligand, *N*-(3-nitrophenyl)-3-phenyl-2-(phenylsulfonamido)propanamide was used as synthesized by Ajani *et al.* [14].

2.1. Synthesis of $La_{0.33}Ca_{0.67}MnO_3$

Manganites were prepared using the sol gel method as described by Iniama *et al.* [15]. In preparing the manganite, 6.25 mmol of La_2O_3 powder (1.357 g) was dissolved in 50 ml nitric acid. 25 mmol $MnCO_3$ (2.8738 g), 12.5 mmol $CaCO_3$ (1.682 g) and 10 g of citric acid monohydrate and 10 ml of ethylene glycol were used in the preparation. The sol gel process of synthesis was followed to yield a dark brown powder. The powder was heated in the furnace at 600ºC for 24 hours and consecutive sintering continued at 900ºC for two hours.

The proposed equation of reaction based on the precursors used is as described below:

$$\frac{1}{6}La_2O_3 + \frac{2}{3}CaCO_3 + MnCO_3 \rightarrow La_{0.33}Ca_{0.67}MnO_3 + CO_2 \uparrow$$

The structural and morphological properties (elemental composition) of the manganite were determined using X-ray Diffractometer (Cu K_α - radiation, PANalytical X'pert Pro MPD diffractometer λ= 1.54056 Å) and JEOL JSM 6400 Scanning Electron Microscopy with magnifications 3000-20,000x coupled to an Energy dispersive X-ray Spectroscopy, respectively.

2.2. Synthesis of citrate capped-LCMO-N-(3-nitrophenyl)-3-phenyl-2-(phenylsulfonamido) propanamide

Trisodium citrate dihydrate, ethanol 99% purity was used as purchased from Sigma Aldrich. All the aqueous solutions were prepared by using a 10mM phosphate buffer solution with pH~7. The trisodium citrate dehydrate was dissolved in 100 mL buffer solution. The funtionalized nanoparticle was synthesized by methods as described by Giri *et al.* [13].

The manganites were rendered soluble by dissolving in a 30 mL of the citrate solution and stirred extensively for 4 hours. The un-reacted nanoparticles were filtered out and the optical properties of the resulting greenish yellow solution was determined using UV-visible Spectrophotometer (Genesys 30 visible spectrophotometer). The *N*-(3-nitrophenyl)-3-phenyl-2-(phenylsulfonamido)propanamide was dissolved in 30 mL of analytical grade ethanol (99% purity). The manganite solution was stirred vigorously for an hour at room temperature to form a homogenous solution. Afterwards, 30 mL of the ligand solution was divided into five aliquots and added to the manganite solution while stirring. The mixture was stirred for about two hours to attain homogeneity of the solution while monitoring with Thin Layer Chromatography (TLC) flexible plates and UV-visible spectrophotometer. The beaker containing the solution was covered with perforated aluminium foil and left undisturbed for 14 days for the crystals to grow. The products were filtered out after 14 days and the recovered products were dried and weighed to obtain the percentage yield thereof. ^{13}C and ^{1}H NMR and SEM-EDS were used in

characterization of the sample. The melting point of both *N*-(3-nitrophenyl)-3-phenyl-2-(phenylsulfonamido)propanamide and citrate capped LCMO-*N*-(3-nitrophenyl)-3-phenyl-2-(phenylsulfonamido)propanamide were determined.

2.3. Antimicrobial properties of the synthesized complex

Prior to the analysis the sample was dissolved in a universal solvent (Dimethyl sulphoxide) (DMSO).The zone of inhibition of the dissolved sample was determined by using the well diffusion method as described by [16, 17]. Nutrient agar was used to sub-culture the microorganisms. The agar was heated so as to convert it to liquid state after which it was cooled to 50ºC in a water bath. Streaks of the *Staphylococcus aureus* (ATCC 25923) and *Pseudomonas aeruginosa* (ATCC 1544) was put into the agar and left alone to set. The petri dish was put in an incubator for 24 hours at 37ºC. Holes of about 5mm to the edge of the plates were drilled into the petri dishes by using a sterile cock borer. 300 mg/mL of the dissolved solution was inoculated into the perforated well using a micro pipette. The petri dish was pre-diffused for 30 minutes and kept in an incubator for 24 hours at 37ºC, until an obvious reduction of the potency of the complex was observed. The zone of inhibition of the sample was determined in mm.10 µg/disc of an antibacterial drug (gentamicin) was used as control.

3. Result and Discussions

3.1. Structural Properties of LCMO

The structural properties of the samples were determined by means of XRD (Fig 1), it was indexed to a perovskite-like structure. The average crystallite size (ΔD) was calculated by using Scherer's formula (Scherer, 1918; Ehi-Eromosele *et al*., 2018).

$$D = \frac{0.9\lambda}{\beta_{FWHM} Cos\theta}$$

The powder x-ray diffraction study showed that most of the sample has a single perovskite phase with identifiable peaks, indexed to the Pnma space group, orthorhombic crystallite structure. The average crystal size was determined as 15.3 nm.

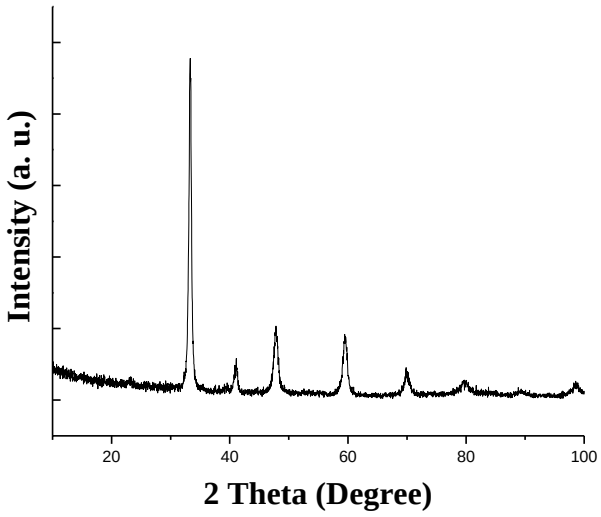

Figure 1. XRD patterns of $La_{0.33}Ca_{0.67}MnO_3$ sintered at 900ºC.

3.2. Morphological properties

The SEM images shown in Figs. 2 (a) – (b) indicated that the manganite was homogenous with the presence of highly porous spherical-like particles. This might be due to the method of preparation (sol gel), which evolved a large amount of gases on ignition. The average elemental composition of the manganite was determined to be $La_{0.32}Ca_{0.68}Mn_{0.97}O_3$. The difference between the nominal composition and the elemental composition might be due to the errors incurred during synthesis of sample.

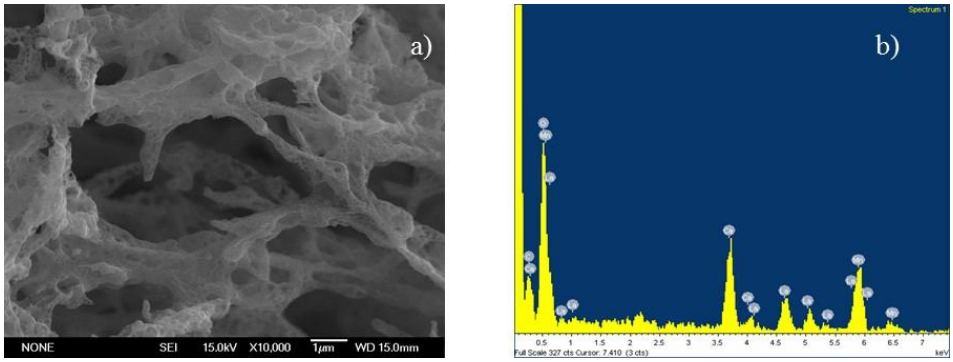

Figure 2. (a) SEM micrograph of LCMO (b) Energy dispersive spectroscopy of showing the elemental composition of LCMO.

3.3. Physical properties of the precursors (citrate capped-LCMO and N-(3-nitrophenyl)-3-phenyl-2-(phenylsulfonamido) propanamide) and the product citrate capped-LCMO-N-(3-nitrophenyl)-3-phenyl-2-(phenylsulfonamido) propanamide

The physical properties of the sample are as described in Table 1. The difference in the melting point of the product and the precursor indicates that a new sample was formed when the citrate capped LCMO reacted with *N*-(3-nitrophenyl)-3-phenyl-2-(phenylsulfonamido) propanamide.

Table 1. Physical properties of citrate capped- LCMO, N-(3-nitrophenyl)-3-phenyl-2-(phenylsulfonamido) propanamide and citrate capped-LCMO-N-(3-nitrophenyl)-3-phenyl-2-(phenylsulfonamido) propanamide.

Precursor	Appearance	Texture	Melting Point (ºC)
Citrate Capped- LCMO	Greenish yellow	Solution	-
N-(3-nitrophenyl)-3-phenyl-2-(phenylsulfonamido) propanamide	Dark orange	Powder	172
Citrate Capped-LCMO-N-(3-nitrophenyl)-3-phenyl-2-(phenylsulfonamido) propanamide	Yellow	Paste	115

3.4. Spectroscopic analysis of the product citrate capped-LCMO-N-(3-nitrophenyl)-3-phenyl-2-(phenylsulfonamido) propanamide

3.4.1 ^{1}H-NMR and ^{13}C-NMR. In view of ensuring that the capped LCMO has indeed been functionalized by the ligand *N*-(3-nitrophenyl)-3-phenyl-2-(phenylsulfonamido) propanamide, ^{13}C-NMR and ^{1}H-NMR were performed in view of determining the alterations that the nanoparticle would induce on its organic ligand. Figs. 3 (a) and (b) show the *^{13}C-NMR* [1] and *H-NMR*, respectively.

^{1}H-NMR (400 MHz, DMSO-d_6) δ_H: 11.09(s, 1H, NH, NH-CO), 8.41-8.39 (d, J = 8.28 Hz, 2H, Ar-H), 8.11-8.04 (dd, J=8 Hz, J_2=28 Hz, 1H, Ar-H), 7.95-7.92 (d, J=9.42Hz, 2H, Ar-H), 7.81-7.78 (m, 1H, Ar-H), 7.65-7.63 (d, J = 7.84 Hz, NH-H), 7.54-7.52(m, 1H, Ar-H), 7.21 (s, 5H, Ar-H), 7.12-7.08 (m, 1H, Ar-H), 3.45-3.40 (q, J = 7.00 Hz, NH-CH-CH_2), 2.10-2.07(d, J = 10.24 Hz, CH_2-CH).

^{13}C-NMR (400MHz, DMSO-d_6) δ_C: 168.9 (C=O), 154.8, 147.9, 141.3 (2 X CH), 135.0, 134.4, 134.2, 132.1 (2 X CH), 120.3, 116.9, 25.4 (CH_2), 24.2 (CH_3) ppm.

The ^{1}H-NMR and ^{13}C-NMR of the compounds were run in DMSO-d_6, the broad shift observed at 4.72 is appropriated to the D_2O, which was used in synthesis of samples. The proton singlet at 7.21 was due to the presence of 5 aromatic protons neighbouring a CH. The suppression of the quartet at 3.45-3.40 might be due to the neighbouring interference of the paramagnetic manganite attached at that site. The ^{13}C-NMR was run at 400 MHz using a deuterated DMSO –d_6 as the solvent. It shows that the presence of 21 carbon atoms with dc ranging from 168.9-24.2, this was made up of aromatic carbons, one aliphatic carbon and one carbonyl group.

3.4.2. Ultraviolet-visible Spectroscopy. Fig. 4 shows the UV-visible spectroscopy of capped LCMO-*N*-(3-nitrophenyl)-3-phenyl-2-(phenylsulfonamido) propanamide and also bare *N*-(3-nitrophenyl)-3-phenyl-2-(phenylsulfonamido) propanamide. The distinct difference between the peaks observed at Fig 3(a) and 3(b) is indicative of the fact that a manipulation had occurred in the ligand. Two broad bands observed at 205 nm and 277 nm were observed in the spectra of the capped LCMO-*N*-(3-nitrophenyl)-3-phenyl-2-(phenylsulfonamido) propanamide while broad bands of 205 nm and 232 nm were observed in the spectrum of bare *N*-(3-nitrophenyl)-3-phenyl-2-(phenylsulfonamido) propanamide, The peaks around 232 nm is assigned to be the $\pi \quad \pi^*$ transition associated with the presence of a benzenoid ring (Ajani *et al*., 2016). The blue shift and broadening of peak at 277 nm might be due to the complex formed between the metal and the *N*-(3-nitrophenyl)-3-phenyl-2-(phenylsulfonamido)propanamide. The similarity in the wavelength observed for both samples might be indicative of the fact that the dominating unit in the complex is the *N*-(3-nitrophenyl)-3-phenyl-2-(phenylsulfonamido)propanamide unit.

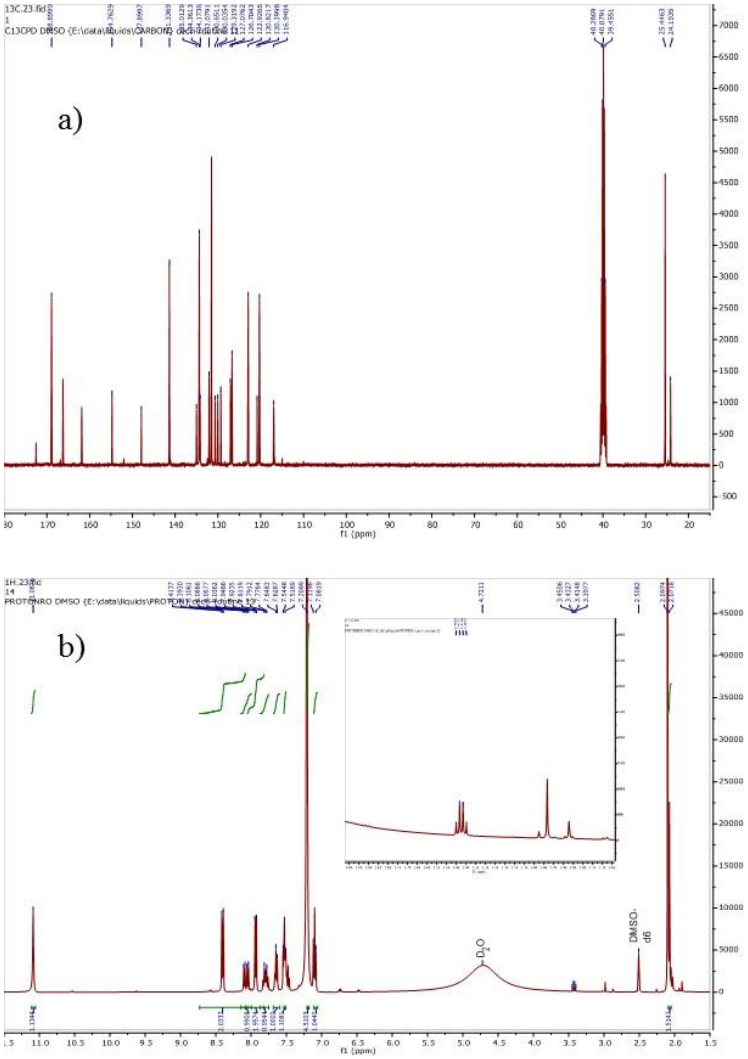

Figure 3. (a) 13C-NMR (b) 1H-NMR of LCMO-N-(3-nitrophenyl)-3-phenyl-2- (phenylsulfonamido)propanamide.

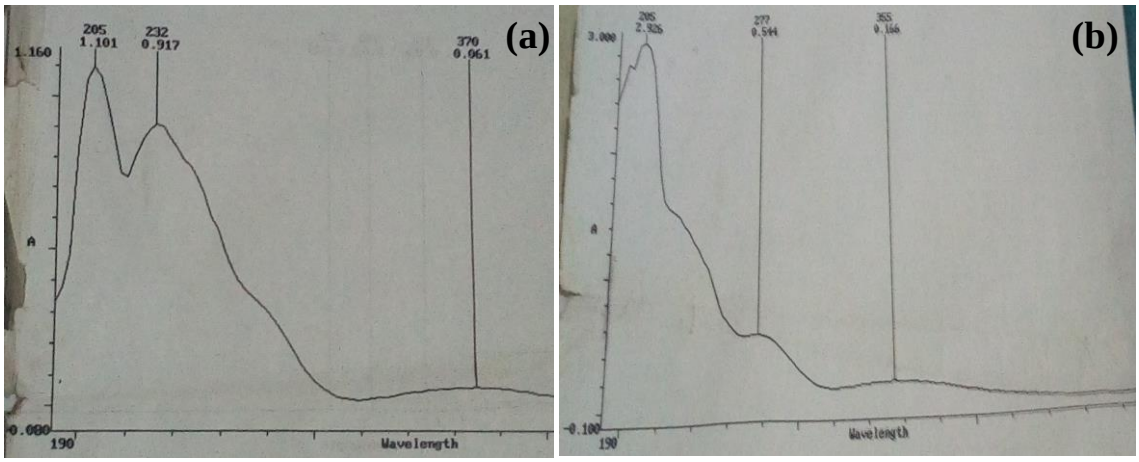

Figure 4. Ultraviolet-visible spectral of (a) NPPA (b) (*N*-(1-((3-nitrophenyl)amino)-1-oxo-3-phenylpropan-2-yl)phenylsulfonamide) manganese.

3.5. Morphological property of citrate capped-LCMO-N-(3-nitrophenyl)-3-phenyl-2-(phenylsulfonamido) propanamide

The morphological property of the product was determined by using SEM. Fig. 5 shows the SEM micrograph of the sample. The morphology of the surface of the sample indicates a film of polymeric aggregation. Although it is known that due to the fact that manganite (LCMO) is a stable compound in aqueous solutions of pH ≤ 6 with no modifications to its initial formulation [13], therefore the film of polymeric aggregation observed on the surface of the metal-citrate nanopartile may be due to the change in the change in the structural formulation of the ligand due to the complex formed with the nanoparticles.

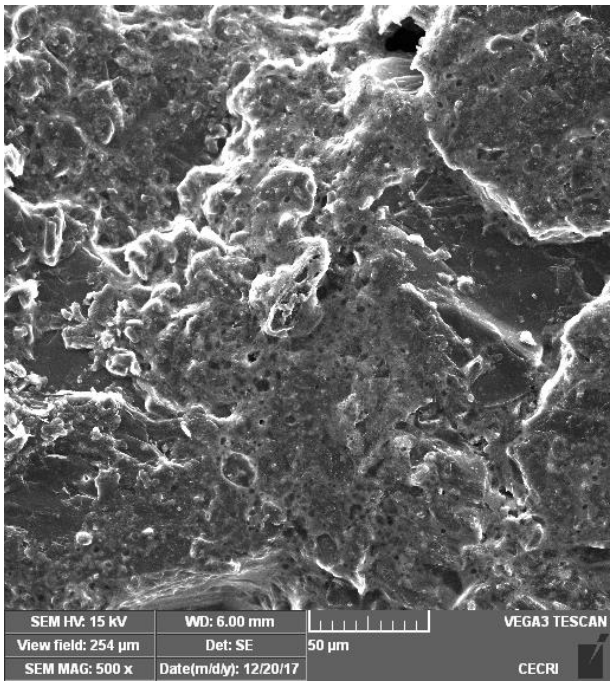

Figure 5. Ultraviolet-visible spectral of LCMO-*N*-(3-nitrophenyl)-3-phenyl-2-phenylsulfonamido) propanamide.

3.6. Antimicrobial analysis of capped LCMO- N-(3-nitrophenyl)-3-phenyl-2-(phenylsulfonamido) propanamide

The sensitivity test (zone of inhibition, mm (ZOI)) of the synthesized complex was determined using the well diffusion method [16]. The two organisms used in this *in vitro* antibacterial analysis were *Staphylococcus aureus*, (gram positive) and *Pseudomonas aeruginosa* (gram negative). From the result obtained, the activities of the complex on the test organisms were classified based on the size of zone of inhibition. It was observed that the product was significantly active with remarkable zone of inhibition against (*Staphylococcus aureus*) with ZOI of 14 nm, and no zone of inhibition against *Pseudomonas aeruginosa*. The resistance of *Pseudomonas aeruginosa* may be due to reduced cell wall permeability of LCMO-*N*-(3-nitrophenyl)-3-phenyl-2-(phenylsulfonamido)propanamide.

4. Conclusion

Manganite, $La_{0.33}Ca_{0.67}MnO_3$ was synthesized at 900ºC using sol gel method. The morphological properties of the resulting brown powder was determined using SEM and TEM. The manganite was capped using citrate and functionalized using *N*-(3-nitrophenyl)-3-phenyl-2-(phenylsulfonamido) propanamide. Optical spectrophotometer (UV-Visible) was used in determining the optical bands of the functionalized sample. Surface morphology of the functionalized sample was determined using SEM.

^{1}H-NMR and ^{13}C-NMR was utilized in determining the alterations of the chemical shifts due to functionalization with the organic ligand. The antibacterial properties of the sample was done against *Staphylococcus aureus* and *Pseudomonas aeruginosa*, it was active against *Staphylococcus aureus* only.

Acknowledgements
We would like to acknowledge Applied Magnetism Institute, Laz Rosaz, Madrid, for granting us the use of their equipment for this research and also Covenant University, Ota, Ogun State, for funding the research.

References
[1] McBain S C, Yiu H H and Dobson J 2008 Magnetic nanoparticles for gene and drug delivery *Int. J. Nanomedicine* **3** 2 169
[2] Akinsiku A A, Dare E O, Ajanaku K O, Adekoya J A, Alayande S O and Adeyemi A O 2016 Synthesis of silver nanoparticles by plant-mediated green method: optical and biological properties *J. Bionanoscience* **10** 3 171-80
[3] Xin Y, Yin M, Zhao L, Meng F and Luo L 2017 Recent progress on nanoparticle-based drug delivery systems for cancer therapy *Cancer Biol. Med.* **14** 3 228
[4] Soppimath K S, Aminabhavi T M, Kulkarni A R and Rudzinski W E 2001 Biodegradable polymeric nanoparticles as drug delivery devices *J. Control. Release* **70** 1-2 1-20
[5] Soni H, Kumar N, Patel K and Kumar R 2017 Metallic Nanoparticles as Alternative Antimicrobials *J. Nanomed. Res.* **6** 4 00165
[6] Sharma A, Goyal A K and Rath G 2018 Recent advances in metal nanoparticles in cancer therapy *J. Drug Target.* **26** 8 617-32
[7] Wilczewska A Z, Niemirowicz K, Markiewicz K H and Car H 2012 Nanoparticles as drug delivery systems *Pharmacol. Rep.* **64** 5 1020-37
[8] Asl H M 2017 Applications of Nanoparticles in Magnetic Resonance Imaging: A Comprehensive Review *Asian J. Pharmaceutics* **11** 1 S7-S13
[9] Hu P, Chen L, Kang X and Chen S 2016 Surface functionalization of metal nanoparticles by conjugated metal–ligand interfacial bonds: impacts on intraparticle charge transfer *Acc. Chem. Res.* **49** 10 2251-60
[10] Schulz F, Friedrich W, Hoppe K, Vossmeyer T, Weller H and Lange H 2016 Effective PEGylation of gold nanorods *Nanoscale* **8** 13 7296-308
[11] Mout R, Moyano D F, Rana S and Rotello V M 2012 Surface functionalization of nanoparticles for nanomedicine *Chem. Soc. Rev.* **41** 7 2539-44
[12] Thiruppathi R, Mishra S, Ganapathy M, Padmanabhan P and Gulyás B 2017 Nanoparticle functionalization and its potentials for molecular imaging *Adv. Sci.* **4** 3 1600279
[13] Giri A, Makhal A, Ghosh B, Raychaudhuri A and Pal S K 2010 Functionalization of manganite nanoparticles and their interaction with biologically relevant small ligands: Picosecond time-resolved FRET studies *Nanoscale* **2** 12 2704-9
[14] Ajani O O, Owolabi F E, Jolayemi E G, Olanrewaju I O and Aderohunmu D V 2017 Facile Synthesis and Spectroscopic Characterization of Sulfonamide Bearing Diversified Carboxamide and Hydrazine Carboxamide Moieties *Rasayan J. Chem.* **10** 4 1412-1
[15] Iniama G, de la Presa P, Alonso J, Multigner M, Ita B, Cortés-Gil R, Ruiz-González M, Hernando A and Gonzalez-Calbet J 2014 Unexpected ferromagnetic ordering enhancement with crystallite size growth observed in La0. 5Ca0. 5MnO3 nanoparticles *J. App. Phys.* **116** 11 113901
[16] Russell A and Furr J 1977 The antibacterial activity of a new chloroxylenol preparation containing ethylenediamine tetraacetic acid *J. App. Bacteriol.* **43** 2 253-60
[17] Geetha R and Roy A 2013 In Vitro Evaluation of Anti Bacterial Activity Three Herbal Extracts on Methicillin Resistant Staphylococcus aureus [MRSA] *J. Pharm. Sci. Res.* **5** 10 207